InAs/GaAs Quantum-Dot Superluminescent Light-Emitting Diode Monolithically Grown on a Si Substrate

Siming Chen,*,[†],[⊥] Mingchu Tang,[†],[⊥] Qi Jiang,[†] Jiang Wu,[†] Vitaliy G. Dorogan,[‡] Mourad Benamara,[‡] Yuriy I. Mazur,[‡] Gregory J. Salamo,[‡] Peter Smowton,[§] Alwyn Seeds,[†] and Huiyun Liu[†]
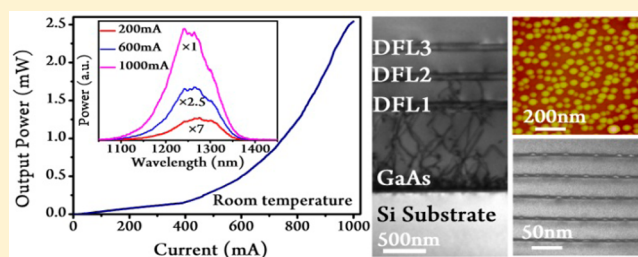
[†]Department of Electronic and Electrical Engineering, University College London, London WC1E 7JE, United Kingdom
[‡]Institute for Nanoscience and Engineering, University of Arkansas, Fayetteville, Arkansas 72701, United States
[§]School of Physics and Astronomy, Cardiff University, Cardiff CF24 3AA, United Kingdom

ABSTRACT: Building optoelectronic devices on a Si platform has been the engine behind the development of Si photonics. In particular, the integration of optical interconnects onto Si substrates allows the fabrication of complex optoelectronic circuits, potentially enabling chip-to-chip and system-to-system optical communications at greatly reduced cost and size relative to hybrid solutions. Although significant effort has been devoted to Si light generation and modulation technologies, efficient and electrically pumped Si light emitters have yet to be demonstrated. In contrast, III−V semiconductor

devices offer high efficiency as optical sources. Monolithic integration of III−V on the Si platform would thus be an effective approach for realizing Si-based light sources. Here, we describe the first superluminescent light-emitting diode (SLD) monolithically grown on Si substrates. The fabricated two-section InAs/GaAs quantum-dot (QD) SLD produces a close-to-Gaussian emission spectrum of 114 nm centered at ~1255 nm wavelength, with a maximum output power of 2.6 mW at room temperature. This work complements our previous demonstration of an InAs/GaAs QD laser directly grown on a Si platform and paves the way for future monolithic integration of III−V light sources required for Si photonics.

KEYWORDS: quantum dot, superluminescent light-emitting diode, Si photonics, monolithic integration

T he development of Si photonics is motivated largely not only by the desire for more diverse, higher functionality, and low cost silicon-based photonic integrated circuits but also by pin count and power dissipation for communications.[1] Although rapid progress has been achieved in Si-based light detection and modulation technologies,[2−4] an electrically pumped Si light-emitting source has remained elusive because bulk silicon is an indirect band-gap semiconductor and therefore has a very low light emission efficiency. In comparison, III−V compound semiconductors have been the mainstays in photonics for light sources, and this dominance holds for near- and mid-infrared wavelengths. Direct integration of III−V semiconductor lasers on Si substrates is one of the best candidate technologies for the realization of an electrically pumped light source on a Si platform, and impressive results have been demonstrated.[5−10] Recently, III−V semiconductor superluminescent light-emitting diodes (SLDs) have also attracted considerable attention. The unique combination of high power and large spectral bandwidth has led to the adoption of SLDs as reliable photonic components for a wide range of applications, such as optical coherence tomography,[11] optical fiber-based sensors,[12] wavelength-division multiplexing systems,[13] and external cavity lasers.[14] In comparison with semiconductor lasers, the advantages of SLDs are their reduced cost, small size, simplified design, ease of operation, and the absence of a fiber connection (for certain designs) with other

photonic components, which can reduce the integration volume. Therefore, there is no doubt that integrating high-performance III−V SLDs monolithically on silicon substrates would further enrich the silicon photonics toolbox, enabling realization of low-cost, massively scalable, high-functionality, and streamlined on-chip light sources.[15]

However, one of the major problems facing the direct monolithic integration of III−V materials on Si is the formation of high-density threading dislocations introduced by large lattice mismatch and the difference in thermal expansion coefficient between III−V epilayers and Si substrates.[1,15,16] Threading dislocations propagating through the active region form nonradiative recombination centers, which led to a deterioration of the performance. To overcome this, a buffer layer between the Si and III−V active region has widely been utilized to reduce the density of threading dislocations.[16] Recently, III−V quantum-dot (QD) devices have attracted significant attention for practical III−V/Si photonics due to their unique properties, in particular less sensitivity to nonradiative defects and delta-function density of states.[5,17] In addition, self-assembled QDs grown by the Stranski−Krastanow (S-K) method have been regarded as a particularly

exciting material system for SLDs because of their naturally occurring large size inhomogeneity.[18] Here, we report on the demonstration of the first III–V QD SLD grown on a Si substrate using InAlAs/GaAs dislocation filter layers (DFLs). The device exhibits a 3 dB bandwidth of 114 nm centered at ~1255 nm with maximum emitted power of 2.6 mW at room temperature.

The III–V InAs/GaAs QD materials were grown by solid-source molecular beam epitaxy (MBE), where the epitaxial growth takes place on n-doped Si(100) substrates with 4° offcut to the [011] plane. Oxide desorption was performed by holding the Si substrate at a temperature of 900 °C for 10 min. Epitaxy was then carried out in the following order: a 30 nm GaAs nucleation layer at 400 °C with a low growth rate of 0.1 monolayer (ML)/s, a 970 nm GaAs buffer layer with a high growth rate of 0.7 ML/s at high temperature, InAlAs/GaAs dislocation filter layers, a 100-period GaAs/AlGaAs superlattice, an undoped active region embedded between two 100 nm GaAs layers, a 50 nm AlGaAs layer grown at 610 °C, and finally, a 50 nm GaAs cap layer. For the growth of the InAlAs/GaAs DFLs, three repeats of five periods of a 10 nm $In_{0.15}Al_{0.85}As$/10 nm GaAs superlattice were used; the three layers of DFLs were each separated by a 400 nm GaAs barrier. For the growth of the active region, five InAs/InGaAs dot-in-a-well (DWELL) layers were grown. Each DWELL layer was formed by depositing 3 MLs of InAs on a 2 nm $In_{0.15}Ga_{0.85}As$ layer, capped with a 6 nm $In_{0.15}Ga_{0.85}As$ layer. The five DWELLs were each separated by a 45 nm GaAs barrier layer, of which the initial 5 nm was grown at 520 °C, and the remaining 40 nm of spacer layer was grown at an elevated temperature of 580 °C to form high-growth temperature spacer layers (HGTSLs). The use of such HGTSLs has been demonstrated to reduce the density of defects and dislocations, improving the optical properties of the stacked layers.[19] Also, in contrast to the growth of QDs for laser structures,[20] here the growth conditions were intentionally offset from the optimized conditions used during the formation of the QDs in order to obtain a high dot density and large size inhomogeneity,[21] which has great advantages for achieving high power and broad bandwidth.

Figure 1 compares the low-temperature photoluminescence (PL) spectra of InAs/GaAs QDs samples with the grown conditions optimized for lasers and SLDs. It is clear to see that the InAs/GaAs QDs grown for SLDs exhibit a broad PL emission bandwidth of 90 nm and much wider than that grown with growth conditions optimized for a laser structure, which has a PL spectrum bandwidth of only 33 nm. Atomic force microscopy (AFM) measurements were also performed on uncapped InAs QDs for morphological study. A typical AFM image for the sample with the growth parameters optimized for broad emission is shown in the inset of Figure 1, from which a large QD size inhomogeneity has been achieved, which accounts for the broader PL bandwidth.

To understand the effects of InAlAs/GaAs strained-layer superlattices (SLSs) serving as DFLs, transmission electron microscopy (TEM) measurements with low magnification were performed as shown in Figure 2a. High densities of dislocations are generated at the GaAs/Si interface due to the large lattice mismatch between GaAs and Si. Most of the defects are confined within 200 nm of the GaAs/Si interface due to the two-step low-temperature growth, but unfortunately a high density (~10^9 cm^{-2}) of threading dislocations continues to propagate into the III–V buffer layer. Thanks to the InAlAs/
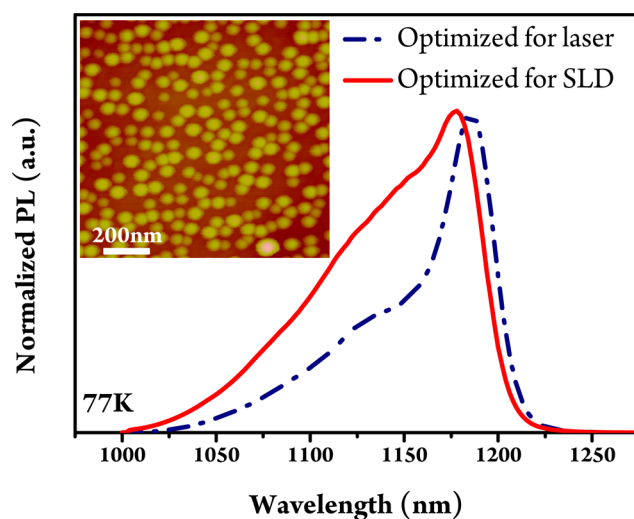

Figure 1. Normalized PL spectra of the InAs QDs with the growth parameters optimized for laser structure and SLD structure at 77 K. The inset shows the AFM image (1 μm × 1 μm) of uncapped InAs QDs optimized for broadband emission.
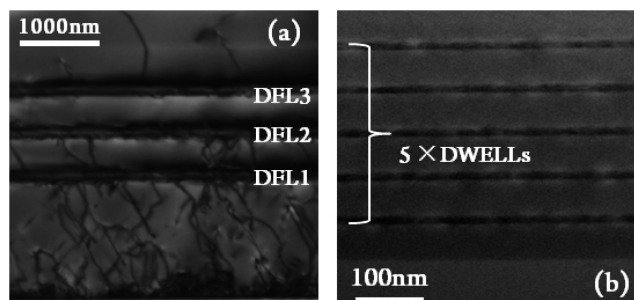

Figure 2. Cross-sectional TEM imaging showing (a) the defect reduction provided by three sets of InAlAs/GaAs DFLs and (b) the active region of the InAs/GaAs QD structure grown on a Si substrate.

GaAs SLS DFLs, after two sets of InAlAs/GaAs SLSs, the III–V GaAs layers are visibly dislocation free, which suggests that the InAlAs/GaAs SLSs can effectively filter/block the propagation of the threading dislocations governed by the misfit strain (that arises from adjacent layers) by redirecting the threading dislocations away from the growth plane.[22,23] Etch pit defect (EPD) measurements were also carried out to probe defect density in a large area, and the results show that, after three sets of InAlAs/GaAs SLSs, the average defect density can be significantly reduced from ~10^9 cm^{-2} to ~10^6 cm^{-2}. Figure 2b shows a cross-sectional TEM image of the active region grown on a Si substrate. It is clear that no obvious dislocation can be observed.

On the basis of the optimized conditions, an InAs/GaAs QD laser structure was developed on a Si substrate with the buffer and active regions of the SLD device grown with the same conditions as the test sample described above. A p-doped upper cladding layer and n-doped lower cladding layers of 1.5 μm $Al_{0.4}Ga_{0.6}As$ were used to confine the five-layer DWELL structures. A 300 nm p-doped GaAs contact layer completed the growth. To evaluate the performance of the QD active element grown on Si, broad-area lasers with a 50 μm ridge-waveguide were fabricated. Devices of 3 mm length with as-cleaved facets were mounted and wire bonded on ceramic tiles to enable testing. Figure 3 shows the single-facet output power
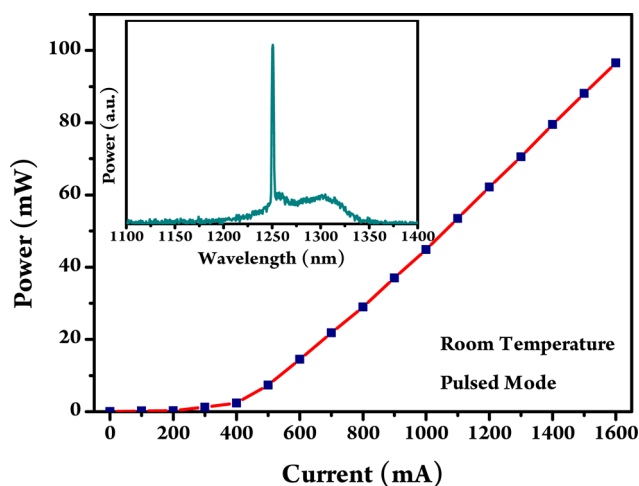
Figure 3. $L-I$ characteristics of an InAs/GaAs QD laser grown on a Si substrate under pulsed operation at room temperature. The inset shows the lasing spectrum just above the threshold.

Figure 5. $L-I$ characteristics of an InAs/GaAs QD SLD directly grown on a Si substrate under pulsed operation at room temperature. The inset shows the output power as a function of temperature.

against current density under pulsed operation of a 1% duty cycle and a 1 μs pulse width at room temperature. A threshold current density of $\sim$330 A/cm^2 is observed, which is lower than previous reported values[6,24] of QD lasers directly grown on a Si substrate. The inset of Figure 3 shows the lasing spectrum just above the threshold, in which room-temperature lasing at $\sim$1.25 μm is clearly observed. These results show the good quality of the QD active media directly grown on the Si substrate.

The SLDs were fabricated in a two-section ridge-waveguide structure following standard ridge-waveguide laser processing. Ridges of 20 μm width were defined by wet etching to a depth of 1.6 μm (i.e., 200 nm above the active region). Two sections were electrically isolated by shallow etch of a highly p-doped GaAs contact layer, providing a resistance of $\sim$2 kΩ between adjacent contacts. Ti/Pt/Au and InGe/Au metal contact layers were deposited on the p-GaAs contacting layer and the exposed n-GaAs buffer layer, respectively. A schematic of the two-section SLD is shown in Figure 4. The device consists of a 2 mm long gain section and a 1 mm long absorber, which was reversely biased to inhibit lasing, while electrically driving the gain section. No facet coating was applied.

Figure 5 shows the $L-I$ curve of the InAs/GaAs QD SLD grown on a Si substrate at room temperature with no active cooling. The device was bar-tested and directly probed without
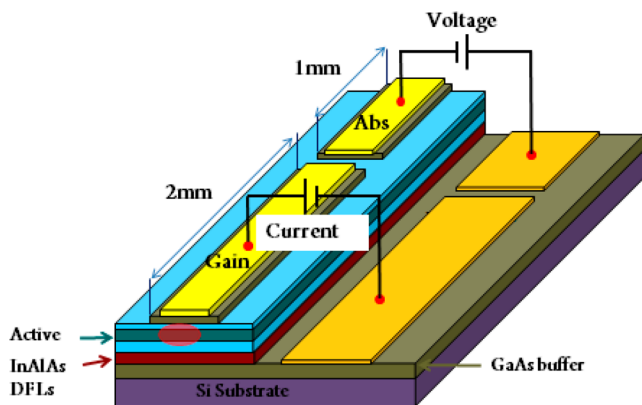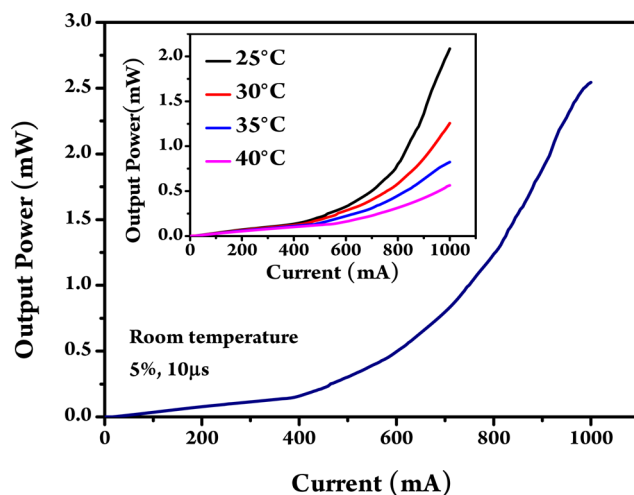
any mounting and bonding. The measurements were taken by electrically pumping the 2 mm long gain section under pulsed operation (5% duty cycle and 10 μs pulse width) with the 1 mm long absorber reversely biased at a voltage of 1 V, acting as a rear optical absorption region. A clear superluminescent characteristic is evidenced by the superlinear increase in optical power with increasing current. At 1000 mA, a maximum single-facet output power of 2.6 mW is observed. Note that this SLD was processed with as-cleaved facets, and the 4° off-cut Si substrates do not cleave perfectly along the {110} plane, leading to imperfect facet quality. The combined effect of facet polishing[9] and antireflection (AR) coating on the facets can further improve the output power. Temperature-dependent $L-I$ characteristics, ranging from 20 to 40 °C, under pulsed conditions (5%, 10 μs) are shown in the inset of Figure 5. Superluminescent behavior is observed for heat-sink temperatures up to 40 °C with the output power decreasing significantly from 2.6 mW to 0.5 mW. This strong effect of temperature on output power is a roadblock facing SLDs to achieve continuous-wave (CW) operation in this work and is mainly due to carrier escape from the heterostructures and increased nonradiative recombination with increasing temperature. In future devices, these thermal effects could be reduced through refinements of the design including p-doping the QDs,[25,26] using an epi-down mounting process,[27] and further reducing the defect density in the buffer layer.

Figure 6 plots the output power spectrum of the InAs/GaAs QD SLD grown on Si as a function of the injection current under pulsed operation of a 5% duty cycle and a 10 μs pulse width at room temperature. A reverse voltage of 1 V was applied on the absorber, eliminating the optical feedback from the back facet. The spectra are offset for clarity. Integrated intensity is deduced from the output power spectrum, also showing an obvious superluminescent behavior as shown in the inset of Figure 6. The evolution of the full width at half-maximum (fwhm) and the center wavelength versus the injection current are illustrated in Figure 7. At a low injection current of 100 mA, the emission is dominated by the lowest energy levels of the QD ground states (GSs). A broadband emission centered at $\sim$1280 nm with a fwhm of $\sim$101 nm was obtained. The relatively wide GS emission is attributed to the large QD size inhomogeneity due to the relatively low growth
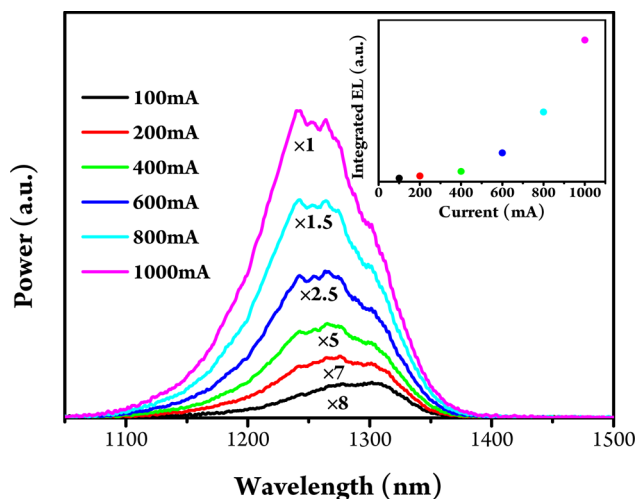

Figure 4. Schematic diagram of the two-section QD SLD device on Si.

Figure 6. Output spectrum as a function of the injection current under pulsed operation (5% duty cycle and 10 μs pulse width) measured at room temperature. The inset plots the integrated intensity measured from the emission spectrum against the injection current.
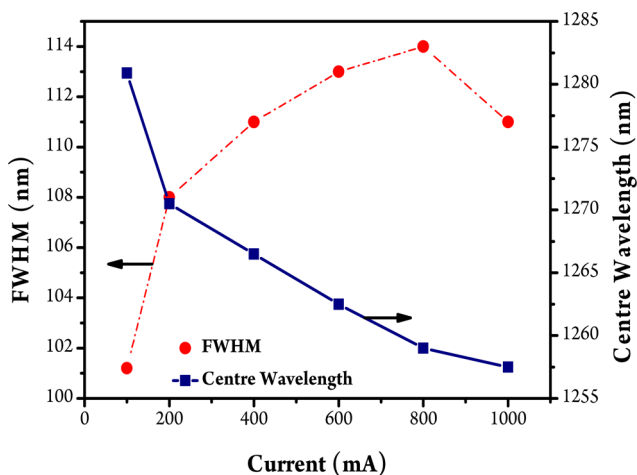

Figure 7. Plots of the evolution of the full width at half-maximum and the center wavelength against the injection current.

temperature and relatively high growth rate used during the formation of InAs QDs. By increasing the injection current from 100 mA to 800 mA, the emission spectrum broadens further to 114 nm with the center wavelength blue-shifted by ~20 to ~1255 nm, which should be attributed to the sequential carrier filling into the high energy levels of small dots' GSs. As the current is further increased to 1000 mA, a reduction in fwhm to 111 nm is observed. This suggests that, at an injection of 800 mA, all the GS energy levels of different sizes of dots are fully populated; that is, an emission spectrum contributed to by all dots' size distributions has been achieved, leading to a maximum fwhm at 800 mA. Above this current, a nonuniform increase in gain for different sizes of dots takes place, resulting in a narrowing of the spectrum line width. In this work, by just optimizing the growth conditions of the active region, a broad emission bandwidth of over 110 nm has been achieved for structures grown on Si. Further improvements in emission bandwidths may be expected through using a combination of chirped QDs,[28] QD intermixing,[29,30] and hybrid QW/QD structures.[31,32]

In conclusion, we have demonstrated the first operation of a III−V QD SLD directly grown on a Si substrate. By carefully controlling the growth parameters as well as utilizing InAlAs/GaAs SLSs acting as DFLs, an emission spectrum of 114 nm centered at ~1255 nm with a maximum corresponding output power of 2.6 mW has been achieved at room temperature from a two-section device. The device performance reported here indicates that the high density of threading dislocations introduced by the large lattice mismatch between the III−V material and the Si substrate is not a fundamental barrier limiting monolithic integration of III−V photonic components on a silicon platform. Most importantly, the work presented here for growing active III−V components on Si substrates is very promising for Si photonics and opens the door toward future monolithic integration of other III−V devices on Si substrates.

■ AUTHOR INFORMATION

Corresponding Author
*E-mail: siming.chen@ucl.ac.uk.
Author Contributions
[⊥]S. Chen and M. Tang contributed equally to this work.
Notes
The authors declare no competing financial interest.

■ ACKNOWLEDGMENTS

■ REFERENCES

(1) Liang, D.; Bowers, J. E. Recent progress in lasers on silicon. *Nat. Photonics* **2010**, *4*, 511−517.
(2) Reed, G. T.; Mashanovich, G.; Gardes, F. Y.; Thomson, D. J. Silicon optical modulators. *Nat. Photonics* **2010**, *4*, 518−526.
(3) Michel, J.; Liu, J.; Kimerling, L. C. High-performance Ge-on-Si photodetector. *Nat. Photonics* **2010**, *4*, 527−534.
(4) Leuthold, J.; Koos, C.; Freude, W. Nonlinear silicon photonics. *Nat. Photonics* **2010**, *4*, 535−544.
(5) Liu, H.; Wang, T.; Jiang, Q.; Hogg, R.; Tutu, F.; Pozzi, F.; Seeds, A. Long-wavelength InAs/GaAs quantum-dot laser diode monolithically grown on Ge substrate. *Nat. Photonics* **2011**, *5*, 416−419.
(6) Wang, T.; Liu, H.; Lee, A.; Pozzi, A.; Seeds, A. 1.3-μm InAs/GaAs quantum-dot lasers monolithically grown on Si substrates. *Opt. Express* **2011**, *19*, 11381−11386.
(7) Lee, A.; Jiang, Q.; Tang, M.; Seed, A.; Liu, H. Continuous-wave InAs/GaAs quantum-dot laser diodes monolithically grown on Si substrate with low threshold current densities. *Opt. Express* **2012**, *20*, 22181−22187.
(8) Lee, A. D.; Jiang, Q.; Tang, M.; Zhang, Y.; Seeds, A. J.; Liu, H. InAs/GaAs quantum-dot lasers monolithically grown on Si, Ge, and Ge-on-Si substrates. *IEEE J. Sel. Top. Quantum Electron.* **2013**, *19*, 1901107-1−1901107-7.
(9) Liu, A. Y.; Zhang, C.; Norman, J.; Snyder, A.; Lubyshev, D.; Fastenau, J. M.; Liu, A. W.; Gossard, A. C.; Bowers, J. E. High performance continuous wave 1.3 μm quantum dot lasers on silicon. *Appl. Phys. Lett.* **2014**, *104*, 041104-1−041104-4.
(10) Tang, M.; Chen, S.; Wu, J.; Jiang, Q.; Dorogan, V. G.; Benamara, M.; Mazur, Y. I.; Salamo, G. J.; Seeds, A.; Liu, H. 1.3 μm InAs/GaAs quantum-dot lasers monolithically grown on Si substrate using InAlAs/GaAs dislocation filter layers. *Opt. Express* **2014**, *22*, 11528−11535.
(11) Huang, D.; Swanson, E. A.; Lin, C. P.; Shuman, J. S.; Stinson, W. G.; Chang, W.; Hee, M. R.; Flotte, T.; Gregory, K.; Puliafito, C. A.;

Fujimoto, J. G. Optical coherence tomography. *Science* **1991**, *254*, 1178−1181.

(12) Burns, W. K.; Chen, C.; Moeller, R. P. Fiber-optic gyroscope with broad-band source. *J. Lightwave Technol.* **1983**, *LT1*, 98−105.

(13) Park, S. F.; Lee, C. H.; Jeong, K. T.; Park, H. J.; Ahn, J. G.; Song, K. H. Fiber-to-the-home services based on wavelength-division-multiplexing passive optical network. *J. Lightwave Technol.* **2004**, *22*, 2582−2591.

(14) Lv, X. Q.; Jin, P.; Wang, W. Y.; Wang, Z. G. Broadband external tunable quantum dot lasers with low injection current density. *Opt. Express* **2010**, *18*, 8916−8922.

(15) Chen, R.; Tran, T.-T.; Ng, K. W.; Ko, W. S.; Chang, L. C.; Sedgwick, F. G.; Chang-Hasnain, C. Nanolasers grown on silicon. *Nat. Photonics* **2011**, *5*, 170−175.

(16) Yamaguchi, M.; Sugo, M.; Itoh, Y. Misfit stress dependence of dislocation density reduction in GaAs films on Si substrates grown by strained layer superlattices. *Appl. Phys. Lett.* **1989**, *54*, 2568−2570.

(17) Arakawa, Y.; Sakaki, H. Multidimensional quantum well laser and temperature dependence of its threshold current. *Appl. Phys. Lett.* **1982**, *40*, 939−941.

(18) Ebiko, Y.; Muto, S.; Suzuki, D.; Itoh, S.; Shiramine, K.; Haga, T.; Nakata, Y.; Yokoyama, N. Island size scaling in InAs/GaAs self-assembled quantum dot. *Phys. Rev. Lett.* **1998**, *80*, 2650−2653.

(19) Liu, H.; Sellers, I.; Badcock, T.; Mowbray, D.; Skolnick, M.; Groom, K.; Gutierrez, M.; Hopkinson, M.; Ng, J.; David, J. Improved performance of 1.3 μm multilayer InAs quantum-dot lasers using a high-growth-temperature GaAs spacer layer. *Appl. Phys. Lett.* **2004**, *85*, 704−706.

(20) Liu, H.; Childs, D. T. D.; Badcock, T.; Groom, K.; Sellers, I.; Hopkinson, M.; Hogg, R. A.; Robbins, D.; Mowbray, D.; Skolnick, M. High-performance three-layer 1.3-μm InAs-GaAs quantum-dot lasers with very low continuous-wave room-temperature threshold currents. *IEEE Photon. Technol. Lett.* **2005**, *17*, 1139−1141.

(21) Zhang, Z. Y.; Hogg, R. A.; Jin, P.; Choi, T. L.; Xu, B.; Ding, D.; Wang, Z. G. High power quantum-dot superluminescent LED with broadband drive current insensitive emission spectra using a tapered active region. *IEEE Photonics Technol. Lett.* **2008**, *20*, 782−784.

(22) Yang, J.; Bhattacharya, P.; Mi, Z. High-performance In$_{0.5}$Ga$_{0.5}$As/GaAs quantum-dot lasers on silicon with multiple-layer quantum-dot dislocation filters. *IEEE Trans. Electron Devices* **2007**, *54*, 2849−2855.

(23) Gourley, P. L.; Drummond, T. J.; Doyle, B. L. Dislocation filtering in semiconductor superlattice with lattice-matched and lattice-mismatched layer material. *Appl. Phys. Lett.* **1986**, *49*, 1101−1103.

(24) Mi, Z.; Yang, J.; Bhattacharya, P.; Huffaker, D. L. Self-organized quantum dots as dislocation filter layers: the case of GaAs-based laser on silicon. *Electron. Lett.* **2006**, *42*, 121−123.

(25) Sugawara, M.; Usami, M. Quantum dot device handing the heat. *Nat. Photonics* **2009**, *3*, 30−31.

(26) Sandall, I. C.; Smowton, P. M.; Walker, C. L.; Badcock, T.; Mowbray, D. J.; Liu, H. Y.; Hopkinson, M. *Appl. Phys. Lett.* **2006**, *88*, 111113−111113−3.

(27) Li, X.; Jin, P.; An, Q.; Wang, Z.; Lv, X.; Wei, H.; Wu, J.; Wang, Z. Improved continuous-wave performance of two-section quantum-dot superluminescent diodes by using epi-down mounting process. *IEEE Photonics Technol. Lett.* **2012**, *24*, 1188−1190.

(28) Li, H.; Rossetti, M.; Fiore, A.; Occhi, L.; Velez, C. Wide emission spectrum from superluminescent diodes with chirped quantum dot multilayer. *Electron. Lett.* **2005**, *41*, 41−43.

(29) Zhang, Z.; Jiang, Q.; Hopkinson, M.; Hogg, R. A. Effects of intermixing on modulation p-doped quantum dot superluminescent light emitting diodes. *Opt. Express* **2010**, *18*, 7055−7063.

(30) Zhou, K.; Jiang, Q.; Zhang, Z.; Chen, S.; Liu, H.; Lu, Z.; Kennedy, K.; Matcher, S.; Hogg, R. A. Quantum dot selective intermixing for broadband light sources. *Opt. Express* **2012**, *20*, 26950−26957.

(31) Chen, S.; Zhou, K.; Zhang, Z.; Childs, D. T. D.; Hugues, M.; Ramsay, A.; Hogg, R. A. Ultra-broad spontaneous emission and modal gain spectrum from a hybrid quantum well/quantum dot laser structure. *Appl. Phys. Lett.* **2012**, *100*, 041118−041118−3.

(32) Chen, S.; Zhou, K.; Zhang, Z.; Orchard, J.; Childs, D. T. D.; Hugues, M.; Wada, O.; Hogg, R. A. Hybrid quantum well/quantum dot structure for broad spectral bandwidth emitters. *IEEE J. Select. Top. Quantum Electron.* **2013**, *19*, 1900209−1900209−9.